Journal of Basic and Applied Engineering Research
p-ISSN: 2350-0077; e-ISSN: 2350-0255; Volume 3, Issue 2; January-March, 2016, pp. 190-197

http://www.krishisanskriti.org/Publication.html

Structural and Optical Properties of Pr_6O_{11} Doped ZnO thin Films Prepared by the RF Sputtering Method

Sowjanya M.[a*], Jayaganthan R.[a,b], Chowdhruy R.[a,c] and Pamu D.[d]

[a]*Centre of Nanotechnology, Indian Institute of Technology Roorkee, Roorkee 247 667, India*
[b]*Department of* Metallurgical and Materials Engineering*, Indian Institute of Technology Roorkee, Roorkee 247 667, India*
[c]*Department of Civil Engineering, Indian Institute of Technology Roorkee, Roorkee 247 667, India*
[d]*Department of Physics, Indian Institute of Technology Guwahati, Guwahati 781 039, India*
E-mail: [a]sowjiphysics@gmail.com, [b]rjayafmt@iitr.ac.in, [c]crajibfce@iitr.ac.in, [d]pamu@iitg.ernet.in

Abstract—*In the present work, we have deposited Pr_6O_{11} doped zinc oxide thin films by RF magnetron sputtering technique. The structural and Optical properties were examined by varying Ar: O_2 gas ratio. Thin films were deposited on to SiO_2/ substrates by RF-magnetron sputtering at 400^o C temperature. The prepared samples were characterized by X-ray diffraction, EDS, AFM, UV–vis-NIR spectrophotometer. It has been found that all the films deposited were polycrystalline with a hexagonal wurtzite structure and preferentially oriented in the (002) crystallographic direction with a grain size of about 30 nm. The deposition rate, transparency, band gap and particle size are better for the films deposited in argon atmosphere in comparison to Oxygen. They have a typical columnar structure and a very smooth surface. Thin films were found to be dependent on roughness of the film. The roughness (5.06 nm) and grain size angle(102.25°) were found maximum for the film deposited at Ar:O_2 ratio (20:0,15:5,10:10,5:15,0:20). The transmittance was also found ~90% at this particular ratio. The band gap of the film deposited at above mentioned ratio was found to be 5.41 eV*

1. INTRODUCTION

Zinc oxide (ZnO) is a polycrystalline versatile and important semiconductor which has attracted significant attraction because of its characteristic properties like transparency in the visible spectrum, direct band gap, the absence of toxicity, abundance in nature etc. These properties find wide technological applications [1]. It is used in batteries, electrical components such as piezoelectric transducers, phosphors, blue laser diodes and varistors [2]. The term "RE" refers to a group of chemically similar metallic elements that occur naturally, their structural and optical properties and some of the novel applications. As a result, of such difficulty, the discovery of all REs took nearly 160 years (from 1788 to 1941) to be completed. In fact, prior to 1945 long and tedious processes were required to purify the metal from their oxides. However, ion-exchange and solvent extraction method are currently used to produce high purity (99.99% pure) and low cast RE elements [3]. RE elements are characterized by the successive filling of their incomplete 4f and 5f shells. Such reduction of the 4fn shell is ascribed to the imperfect screening of one 4f electron by another 4f electron because of the shape of the orbital. As the number of 4f electrons successively increases by one at each element the nuclear charge rises as well. As a result, the effective nuclear charge experienced by the 4f electrons increases due to poor shielding and hence the 4f electrons tend to be more and more firmly bound to the nucleus causing a reduction in the size of 4f shell [4]. The RE ions interact with the crystal lattice vibrations (knows as phonons) due to the dynamic crystal field which is induced by shifting the neighboring ions from their equilibrium positions and alter the electrical field experienced by the RE ions. Consequently, these perturbation factors will cause some higher states having the different parities to be mixed up with the 4f states making admixtures of states that will permit 4f-related transitions to take place. Such types of transition are called electric dipole forced transitions [5].The Optical properties of RE ions are dominated by the radioactive transition within the 4f manifolds. As a result, a great deal of research has been carried out by many scientists to investigate the RE-related transitions. For example, Duke and co-Workers [6] have intensively investigated the optical transitions of different trivalent lanthanide [7] (LaCl3) bulk crystals and provide us with a very useful energy level diagram which shows the energy of the different (2S+1)LJ states for various RE3+ ions. The relative position of the low-lying 4f energy levels of trivalent lanthanides ions. Although Duke's study was based on systematic spectral measurements of RE ions incorporated into a specific crystal it can still be reliably used as a good qualities description to study the energy levels of RE ions in most crystals. This assumption can be rationalised follows, since the effect of the crystalline field is weak due to the electrostatic shielding effect when the RE ions are incorporated into crystals the spin-orbit interaction between the 4f electrons themselves is dominant with its value largely

independent of the host matrix. Thus, the energy levels of the 4f states of RE ions are slightly perturbed and the gross optical features of RE ions in most solids are expected to be similar to those of the free ions [8]. Many important RE-related applications ranging from high=technology to medicine and health rely principally on the novel physical and chemical properties of RE. For example, the localised 4fn transitions are responsible for the unique optical properties of RE ions which are key components in optical fibres, data storage, high laser power systems, display monitors, energy efficient fluorescent light bulbs, phosphor-based light -emitting diodes and medical imaging [9].They also play a significant role in high-tech digital products that surround us in our daily lives audio-visual equipment, photographic and communication devices[10]. Furthermore, RE elements contribute greatly to the fast growing field of green energy technology which aims to limit gas emissions. In this technology, RE elements are key factors in producing hybrid and electric vehicles and wind power generators, hence minimising hydrocarbon consumption. Re elements are also used as catalysts in the petroleum refining process. They are capable of producing strong permanent magnets that are useful in a wide range of applications. Therefore, RE elements are increasingly considered indispensable and non-replaceable materials.Several studies have been reported on ZnO thin films deposited on various substrates including glass, Si, GaAs and GaN and diamond [11].Essential, the substrate is very important for the growth of thin films in terms of the lattice arrangement and thermal mismatching between it and thin films. The reason is due to the lattice disparity between the films and the substrate generally leads to the residual stress in the deposited films. The doping of ZnO is being considered for manufacturing transparent electrodes thanks their high luminous transmittance, good electrical conductivity, good adhesion to the substrate and the fact that they are chemically inert. In this chapter, transparent conducting Pr-doped ZnO films deposited on Si(100), SiO2, SS-316L substrates at 400oC temperature using RF magnetron sputtering technique. The effect of Ar: O2 partial pressure ratio on structural and optical properties. Doping of ZnO using Pr species, in particular, is more effective for the stabilization of lattice systems and increases the iconicity of chemical bonds in ZnO films. Because of its less toxic in nature and moderate cost.

2. EXPERIMENTAL DETAILS

The target designed by the conventional solid–state method from high–purity ZnO powder (> 99.99%) and Pr6O11 (> 99.99%) nanoparticles. The required materials were mixed according to the stoichiometry of ZnO and ground in distilled water for 5 hours in the ball mill (Fritsch GmbH, Germany). The prepared mixture was dried and calcined at 100 °C for 23 hours in the air. The heated powder was cooled at room temperature and re–milled by adding 3% of Pr6O11 nanoparticles. Further, the powder was added with an organic binder (by adding few drops of PVA) and compressed uniaxially into a 56 mm size in diameter cylindrical target about 4 mm in thickness. Similarly, the pellets were pressed with 10 mm in diameter and 3 mm in thickness. The obtained sputtering target and pellets were sintered at 1000 °C for 3 hours in the air medium. A similar process was used to prepare a target of Pr6O11 doped ZnO. Thin films were deposited on Si(100), SiO2, SS-316L substrates using RF sputtering system using sintered target for further study. The Si(100), SiO2, SS-316L substrates (~1×1 cm in size) were ultrasonically cleaned in distilled water followed by alcohol and then dried prior to the deposition. The substrates were fastened parallel to the sintered target and the shutter was placed between the target and substrate in order to avoid the unwanted sputtering. The sputtering chamber was emptied to the base pressure of 5×10−5 mm Hg before the deposition. The used temperature of the substrate was about 400 °C and the radio frequency power (PRF) of 40 W for deposition. Sputtering was carried out in Ar plasma with a deposition time of 3 hours. Sputtering deposition parameters and materials used were shown in Table 1. The uniform distance was employed between sputtering target and substrate for all the depositions (~4.5 cm), the ratio of sputtering gas Ar to O2 was varied from (20:0, 15:5, 10:10, 5:15, 0:20). Figure 1 represents the flow chart of steps involved in the target preparation Five samples were prepared in Ar: O2 atmosphere by varying Argon to oxygen ratio (20:0,15:5,10:10,5:15,0:20).) and characterization.

Table 1: Sputtering deposition parameters and materials used

Description	*Value or Parameter*
Target prepared:	Pr6O11 doped ZnO
Substrate used:	Si/ SiO2/SS_316L
Base pressure:	2.5×10^{-5} mbar
Working pressure:	3.0×10^{-2} mbar
Power supplied:	40 w
Distance (between target and substrate):	4.5 cm
Temperature:	673 K
Deposition time:	3 h

2.1. Characterization of the thin films

Structural characterizations of these thin films were examined by X-ray diffract meter model (Model: D8 ADVANCE, Brucker) in 2θ mode, with CuKα radiation (λ=0.154 nm). The source of X-ray operated at a power of 40 kV 30 mA. The surface topography and roughness of the as grown films were examined by atomic force microscopy (AFM; NT-MDT: Model NTEGRA) in semi-conduct mode with the silicon nitride tip of radius 10 nm. The grain morphology and the chemical composition from energy dispersive analysis of X-rays (EDX) of the thin film samples was examined by field emission scanning electron microscopy (FESEM; Model: Quanta 200F FEG and FEI Netherlands) with a very high

electric potential of 20 kV. The optical properties transmittance, absorbance and reflectance for these thin films were observed by (Varian Cary 500 UV-VIS NIR) spectrophotometer. The optical band gap was calculated from the Talc's plot $(\alpha h\nu)^2$ versus hν. Photoluminescence (PL) spectra were obtained for the films by using spectrofluorophotometer (SHIMAZDU, Model: RF–5301PC) with 150W xenon lamp, ozone resolving type lamp housing and operating temperature at 25 °C. The light source of Xe lamp at the excitation wavelength of 325 nm was used for PL study. All the measurements were performed in air at room temperature.

3. RESULTS AND DISCUSSIONS

3.1. Structural properties

3.1.1. XRD analysis

Fig. 1(a and b) represents the XRD patterns of Pr_6O_{11} doped ZnO pellets and thin films respectively. Fig. 1(a) represents the XRD plot of Pr_6O_{11} doped ZnO pellets and were sintered at 1050 °C. The XRD peaks of thin film deposited on the SiO_2/Si/SS-316L substrates in Ar:O_2 atmospheres at 400 °C which are shown in the Fig. 1(b). As observed from the Fig 1(b) the XRD patterns were polycrystalline films with hexagonal (wurtzite) structure. It can be also seen that from Fig. 1(b) the intensity for the entire plane remained highest for Pr_6O_{11}-doped ZnO. The diffractogram that the peak at (002) planes dominates the other peaks appearing clearly indicating the superior orientation of thin films or pellet along the *c*-axis. The growth patterns of the Pr_6O_{11} doped ZnO thin films were at right angles to SiO_2/Si/SS-316L substrates.

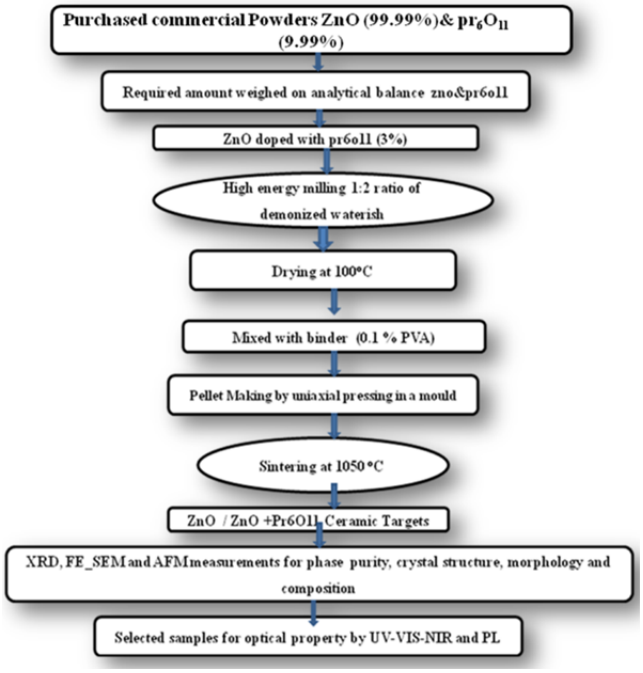

Fig. 1: Flow chart for target preparation.

The polycrystalline films with hexagonal (wurtzite) structure were observed for pellet and doped thin films in the range of 20–80°. The major peak (002) was observed at 34.4° for both Pr_6O_{113} doped ZnO thin films and pellet. The average crystalline sizes of the thin films deposited on SiO_2/Si/SS-316L substrates have been calculated using the Scherer's equation as shown below:

$$D = \frac{0.9\lambda}{\beta\cos\theta} \tag{1}$$

where λ is the wavelength of X-rays used at λ = 0.154 nm, for Cu *Kα* target and θ is the Bragg's diffraction angle of the peak (002). For the hexagonal lattice, lattice spacing *d* is given by the below specified relation:

$$\frac{1}{d^2} = \frac{4}{3}\left(\frac{h^2 + hk + k^2}{a^2}\right) + \frac{l^2}{c^2} \tag{2}$$

where *h*, *k*, and *l* are Miller indices of the plane and *a* and *c* are the lattice constant for the hexagonal unit cell. From Eq (2) values for the lattice constants *a* and *c* are calculated.

3.1.2. FE-SEM and EDX analysis

The field emission scanning microscopic (FE-SEM) study was carried for the surface morphology of the thin film with pr_6O_{11}doped (2 at.%) ZnO and Fig 2 (a) represents the same. From t he Fig. 3.1 (a), very fine grain averaging to near 32 nm are observed and distributed evenly with high uniformity throughout. The uniform distribution is the result of controlled preferential nucleation of the grains drive by RF sputtering deposition process. Films have uniform density and composed of randomly oriented grains. The grains are very smaller and more elongated in thin film prepared with lower pr_6O_{11} concentration. The grain size increases and the shape of the grains become round and hexagonal with increasing precursor concentration as observed in Fig. 3.1(a). Similarly, Fig. 3.1(b) indicates the EDX spectra of pr_6O_{11} doped ZnO thin films prepared by RF sputtering.

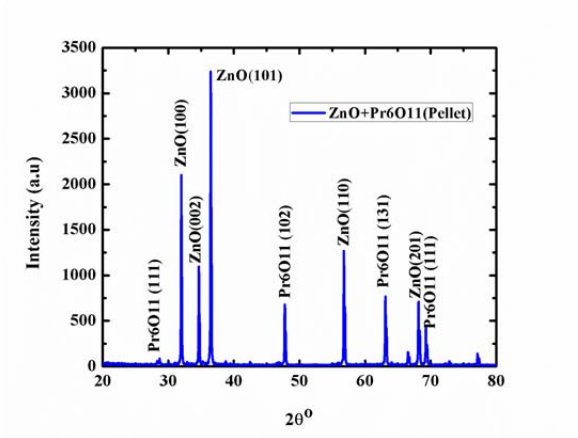

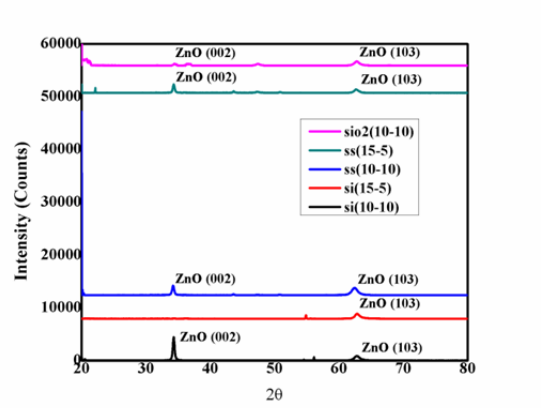

Fig. 2(a). XRD plot of Pr6O11 doped ZnO pellets at 1050 °C. (b). XRD plot of Pr6O11 doped ZnO thin films on Si /SiO2/SS-316L substrate at 400 oC.

The main idea of the EDX analysis in this study is to identify the elements presents in the deposited thin film after the calcination. As observed from Fig. 3.1 (b), the elements such as Zn, Pr and O are present in thin film. Even after calcination of target at ~1000 °C and deposited the thin films at 400 °C by sputtering, elements were remained unchanged which conforms the originally prepared materials in its original state.

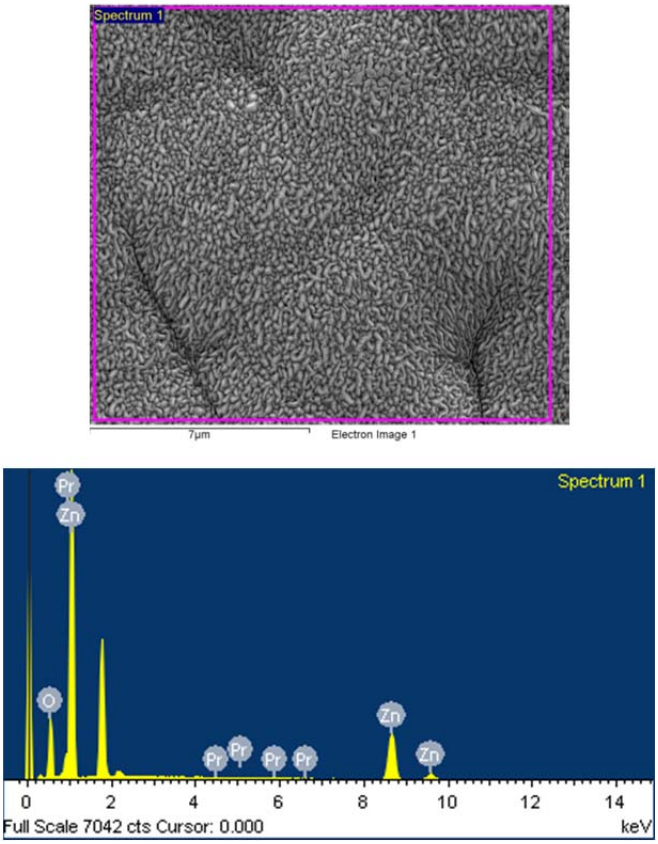

Fig. 3.1. (a) FE-SEM images of Pr6O11doped ZnO thin films deposited on Si substrate at 400°C. (b), Pr6O11doped ZnO thin films deposited on Si substrate at 400 °C.

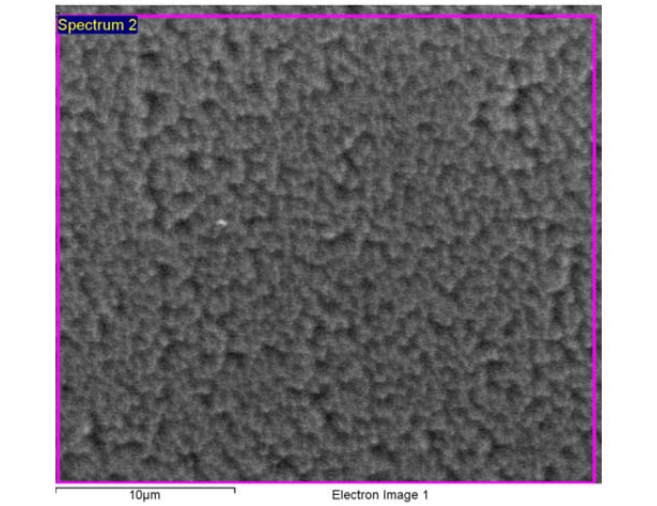

Fig. 3.2. (a), FE-SEM images of Pr6O11doped ZnO thin films deposited on SiO2 substrate at 400oC. (b), Pr6O11doped ZnO thin films deposited on SiO2 substrate at 400 °C.

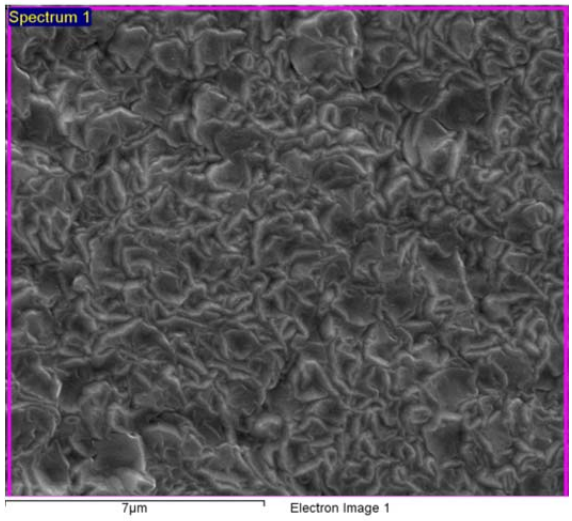

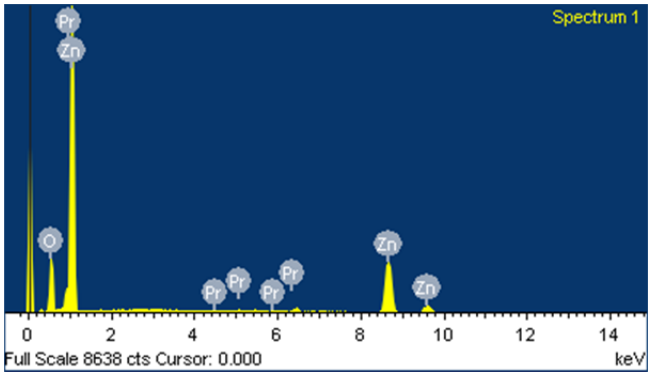

Fig. 3.3. (a) FE-SEM images of Pr6O11doped ZnO thin films deposited on SS-316L substrate at 400oC. (b), Pr6O11doped ZnO thin films deposited on SS-316L Substrate at 400 oC.

3.1.3. AFM analysis

Atomic force microscopy (AFM) was used to study the surface topography of pr_6O_{11} doped ZnO thin films. Fig. 4(a) shows the 2 dimensional AFM image of the sample deposited on SiO_2/Si/SS-316L substrate. The anisotropic grain growth may occur in thin films due to the factors such as preferred orientation of the grains, orientation-dependent grain boundary mobility and grain boundary free energy, and residual stress which gives an excellent measure of the smooth film fabricated with a high homogeneity. As shown in 3D image of the Fig. 4 (b), uniform and homogenous crystallite distribution results in the enchased film transparency. The average roughness is 13.147 nm and RMS 17.385 nm roughness and grain size of the thin film results reported.

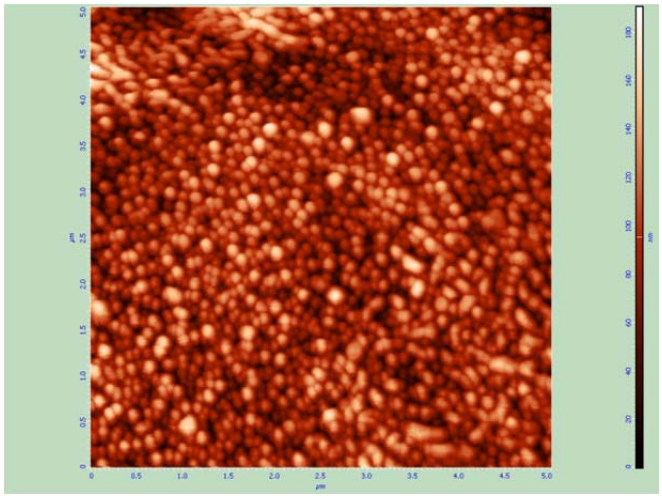

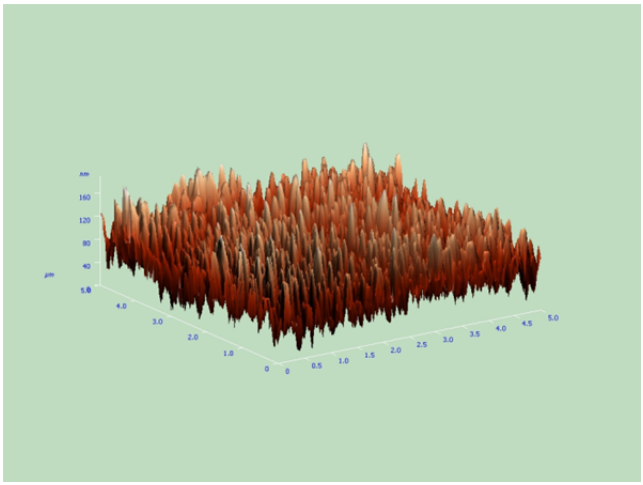

Fig. 4.1. (a), 2D image of Pr6O11 doped ZnO thin film deposited on Si substrate at 400oC. (b), 3D image of Pr6O11 doped ZnO thin film deposited on Si substrate at at 400oC .

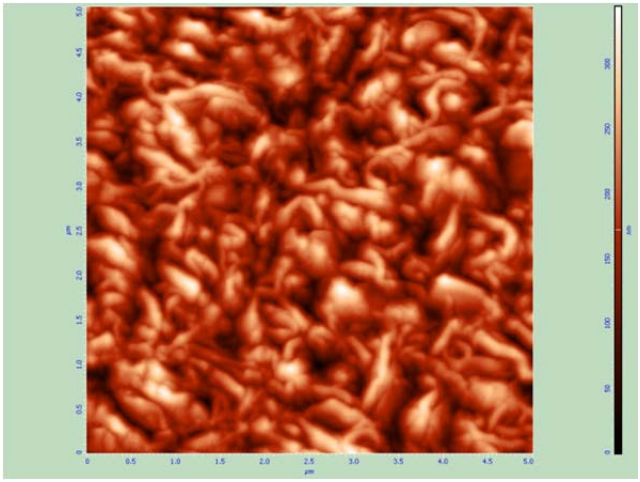

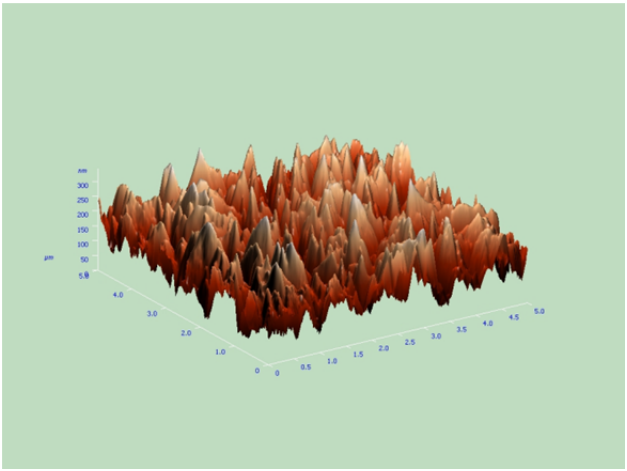

Fig. 4.2. (a), 2D image of Pr6O11 doped ZnO thin film deposited on SiO2 substrate at 400oC. (b), 3D image of Pr6O11 doped ZnO thin film deposited on SiO2 substrate at at 400^o C.

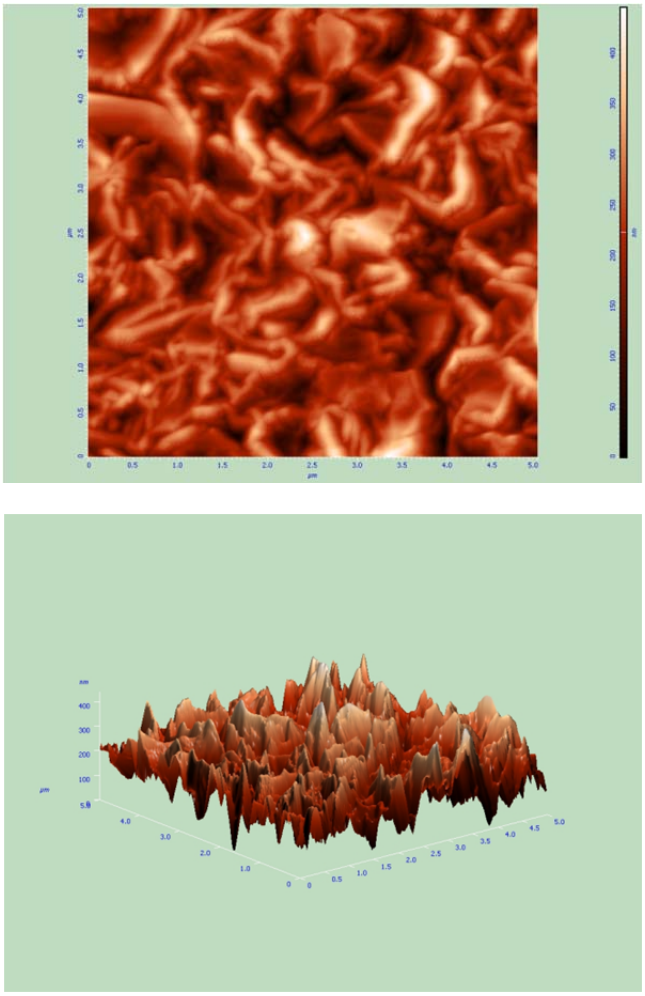

Fig. 4.3. (a), 2D image of Pr6O11 doped ZnO thin film deposited on SS-316L substrate at 400oC. (b), 3D image of Pr6O11 doped ZnO thin film deposited on SS-316L substrate at at 400oC.

3.2. Optical measurement

The optical absorbance is shown in Fig. 5 in the wave length range between 300-800 nm at various Ar:O_2 ratios. The optical absorbance of different Ar:O_2 ratios (20:0), (15:5), (10:10), (5:15), (0:20) between 0 to 50% in near-UV spectral region ranges from 400 nm down to 300 nm. The absorbance less than 50% below the energy band gap, the absorption is caused by the defects states. The absorption edge shifts towards longer wave lengths in the increasing Ar:O_2 ratios the thin film thickness decreasing indicating a decreasing in the band gap. It is also revealed that with increase in argon to oxygen ratio, the absorbance value decreases.

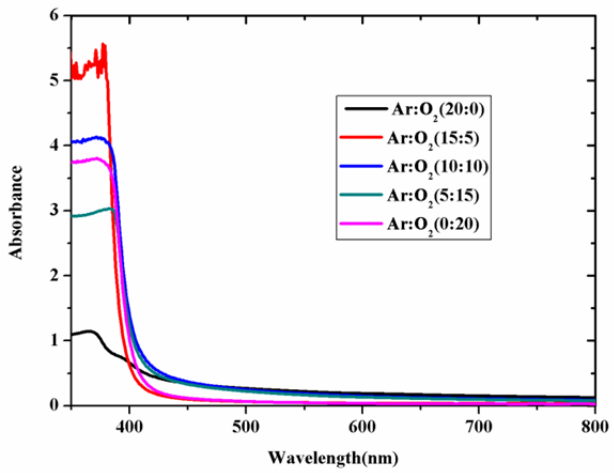

Fig. 5.Plot of Absorbance vs wavelength for Pr6O11doped ZnO thin film on SiO2 substrate at400 oC C different Ar:O2 gas ratios.

The reflectance spectrum is demonstrated in Fig. 6 (b) in the spectra range of 300 to 800 nm. From the figure it is clear that the reflectance quite low in all the samples. The change in optical reflectance may be due to the morphological change in films, as the aspect ratio of crystallites changes with sputtering Ar:O_2 gas ratios decreasing then thin film thickness also in decreasing. The optical transmittance spectra as shown in Fig. 4.(c) in the wave length 300 to 800 nm, the average transmittance achieved in the visible range was very high for various Ar:O_2 gas ratios. These curves show a well defined interference fringe pattern, indicating the smooth surface of the thin films.

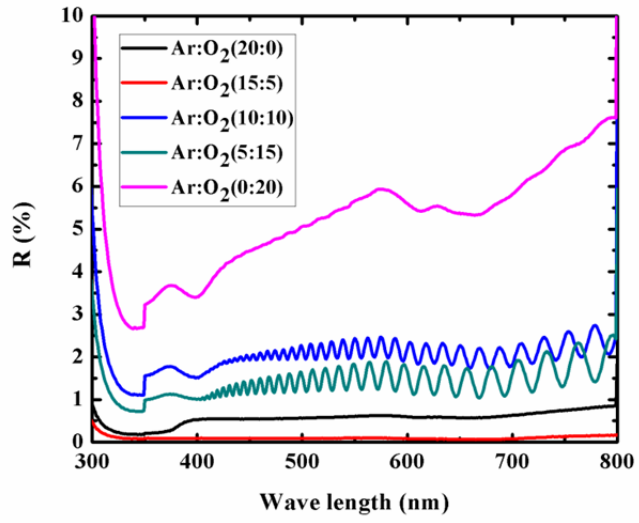

Fig.6.1. (a), Plot of Reflectance vs wavelength for Pr6O11doped ZnO thin film on Si substrate at400 oC C different Ar:O2 gas ratios.

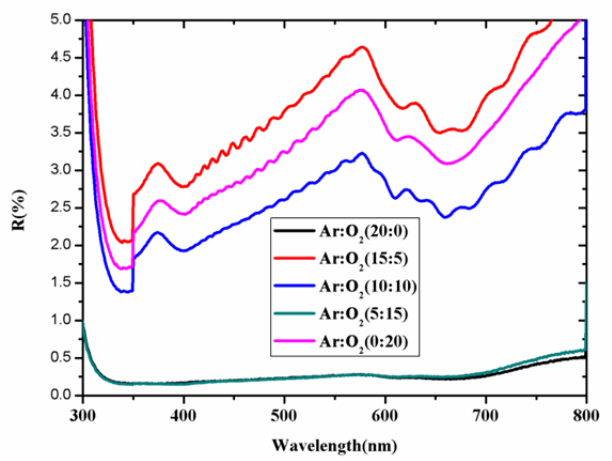

Fig. 6.1. (b), Plot of Reflectance vs wavelength for Pr6O11doped ZnO thin film on SiO2 substrate at400 °C C different Ar:O_2 gas ratios

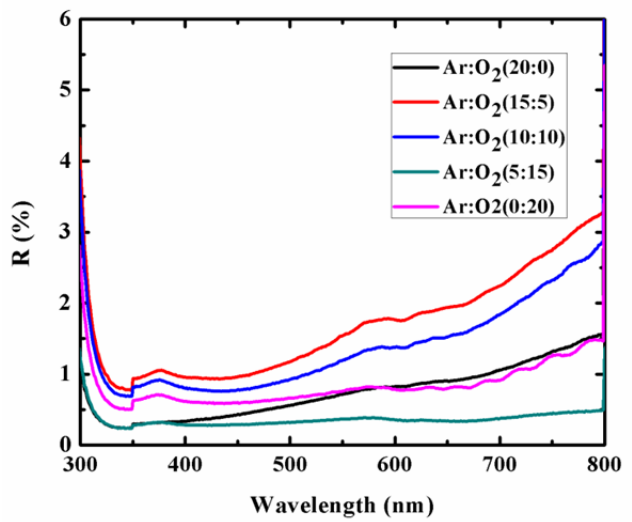

Fig. 6.1: (c), Plot of Reflectance vs wavelength for Pr6O11doped ZnO thin film on SS-316L substrate at400 oC C different Ar:O2 gas ratios.

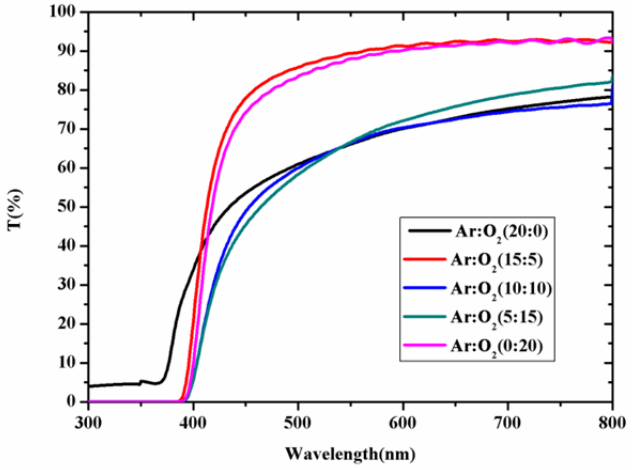

Fig. 7: Plot of transmittance vs wavelength for Pr6O11 doped ZnO thin film on SiO2 substrate at different Ar:O2 gas ratios.

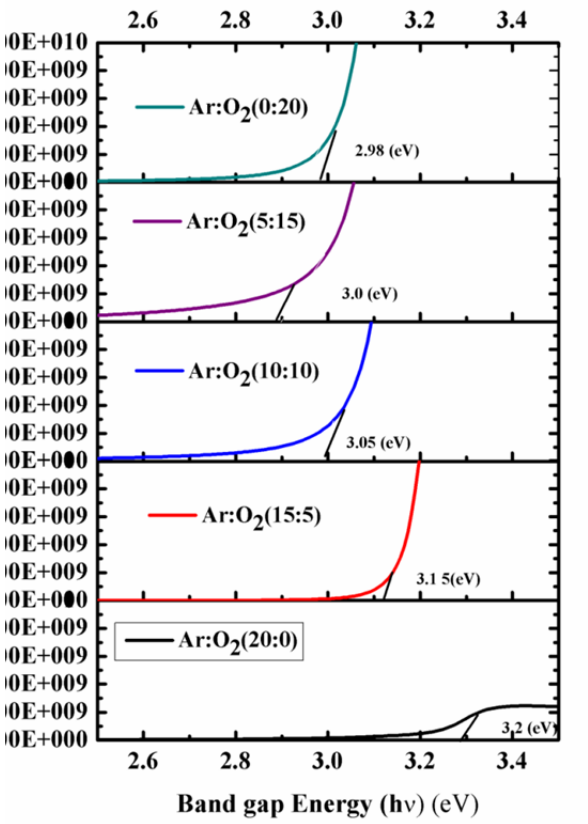

Fig. 8: plot of (αhv)2 vs. hv for Pr6O11doped ZnO thin films with different sputtering gas ratios concentration.

These thin films suitable for application as the window layer for solar cell fabrication and transparent electromagnetic interference (EMI) shielding materials. From the transmittance data absorption coefficient α can be calculated using Lamber's formula [22].

$$\alpha = \frac{1}{t\left[\ln(t/T_r)\right]} \tag{3}$$

where T_r and t are the optical transmittance and thickness of the thin film, respectively. The optical band gap of thin films was calculated. Based on the theory of optical transmission, the relationship between the absorption coefficient (α) and photon energy of the incident light ($h\nu$) for direct transition is given by the below equation:

$$(\alpha h\nu)^n = A(h\nu - E_g) \tag{4}$$

where A is constant, E_g is band gap in eV. For n=1/2 the transition data provide the best linear fit in the band-edge region, implying the transition is direct in nature. The direct band gaps of the films were calculated from the $(\alpha h\nu)^2$ vs. $h\nu$ (Tauc model) plot by extrapolating a fit of the linear region to α= 0, as shown in Fig. 4(d). The linear dependence of $(\alpha h\nu)^2$ with $h\nu$ indicates that Pr_6O_{11} doped ZnO thin films are direct transition type semiconductors. The optical band gap of thin films lies in the range between 3.366 eV and 3.038 eV. The

observed band gap values are almost increased with increasing the argon gas concentration. The values of Pr_6O_{11} doped ZnO thin films deposited at different $Ar:O_2$ ratios are as follows: for 0:20 (2.981 eV), 5:15 (3.0 eV), 10:10 (3.05 eV), 15:5 (3.15 eV), and 20:0 (3.2 eV).

3.3. Photoluminescence (PL)

Photoluminescence (PL) is the emission of the light after the absorption of the electromagnetic radiation. It is generally known that the intensities of the PL spectrum provide the information about the optical band gap, defects and the quality of the deposited films. PL spectra were obtained for all deposited thin films. PL emission studies at room temperature for Pr6O11 doped ZnO thin films with different ($Ar:O_2$) sputtering gas ratios (20:0), (15:5), (10:10), (5:15), (0:20) carried out in the wavelength range of 300 to 600 nm and at the excited wavelength of 330 nm. All the spectra exhibited a broad peak at nearly 389 nm with less intense secondary emission at 400 to 445 nm. The PL intensity was observed to be more for sputtering gas ($Ar:O_2$) ratio for 15:5 out of (20:0), (10:10), (5:15), and (0:20). The defects that are created due to different $Ar:O_2$ gas proportions strongly influence the PL emission. The peak at 350 to 450 nm in all the cases may be due to the prances of the Zn vacancies. The results are in good agreement with the previous PL results on thin films.

4. CONCLUSION

In this study Pr6O11 doped ZnO thin films of varying ($Ar:O_2$) RF sputtering gas ratios were successfully deposited on SiO_2/Si/SS-316L substrates. The deposited thin films are single phased with prudential growth in (002) plane, along the c–axis. Polycrystalline films with hexagonal (wurtzite) structure are observed. The surface topography studies from AFM and FESEM images describe that the grains are uniformly grown on the film surface. The surface of thin films is reasonably smooth with small values of average and RMS roughness. The deposited thin films show good optical characteristics, very high optical transmittance in the visible region, low optical reflection exhibit a sharp absorption edge at a wavelength below 400 nm, hence Pr_6O_{11} doped ZnO lowers the band gap. The large values of optical transmittance enable application of Pr_6O_{11} doped ZnO thin films for transparent window layer of solar cells. Photoluminescence (PL) spectra show sharp peaks in the UV and visible regions. Due to visible emission peaks Pr_6O_{11} doped ZnO thin films find optical applications such as LEDs, window layer for solar cell fabrication and transparent electromagnetic interference (EMI) shielding materials, and laser diodes. The Pr_6O_{11}-doped ZnO thin films exhibit excellent optical properties, and are applicable for fabrication of optoelectronic devices.

5. ACKNOWLEDGEMENTS

The authors thank CSIR for financial support as JRF/SRF fellowship. We also thank Computer Center, Mahatma Gandhi Central Library and Institute Instrumentation Centre of IIT Roorkee for providing necessary facilities. SM extends her acknowledgments to IIT Guwahati for providing experimental facilities. Sincere thanks to Mr. Mahesh, Ms. Pallabi, Mr. Anil Kumar, Dr. P. Rajendra and Dr. T. Santosh Kumar for their help and support during experimentation

REFERENCES

[1] Look, D. C. Recent advances in ZnO materials and devices. *Materials Science and Engineering B: Solid-State Materials for Advanced Technology*, *80*(1-3), (2001). 383–387.

[2] Fernández Hevia, D., Caballero, a. C., de Frutos, J., & Fernández, J. F. Dominance of deep over shallow donors and the non-Debye response of ZnO-based varistors. *Journal of the European Ceramic Society*, *25*(12 SPEC. ISS.), (2005). 3005–3009.

[3] David R Lide, E. CRC Handbook of Chemistry and Physics, Internet Version 2005. *CRC Press, Taylor and Francis Boca Raton FL*, 0. (2005).

[4] Hanna, D.. Rare-earth-doped fiber lasers and amplifiers, 2nd edition. *Optics and Lasers in Engineering*. (2003).

[5] Becker, P. C., Olsson, N. A., & Simpson, J. R. *Erbium-Doped Fiber Amplifiers*. *Erbium-Doped Fiber Amplifiers*. (1999).

[6] Dieke, G. H., Crosswhite, H. M., & Dunn, B. Emission Spectra of the Doubly and Triply Ionized Rare Earths. *Journal of the Optical Society of America*, *51*(8), 820. Gschneidner, K. A., Bünzli, J.-C. G., & Pecharsky, V. K. (2005). Handbook on the Physics and Chemistry of Rare Earths Vol. 35. In *Journal of Alloys and Compounds* (Vol. 255, pp. v–ix). (1961).

[7] Gschneidner, K. A., Bünzli, J.-C. G., & Pecharsky, V. K. Handbook on the Physics and Chemistry of Rare Earths Vol. 35. In *Journal of Alloys and Compounds* (Vol. 255, (2005). pp. v–ix).

[8] Comby, S., & Bünzli, J. C. G. Chapter 235 Lanthanide Near-Infrared Luminescence in Molecular Probes and Devices. *Handbook on the Physics and Chemistry of Rare Earths*, *37*(07), (2007). 217–470.

[9] Bunzli. *Spectroscopic Properties of Rare Earths in Optical Materials*. *Materials Science* (Vol. 83). (2005).

[10] Myslinski, P., Szubert, C., Bruce, A. J., DiGiovanni, D. J., & Palsdottir, B. Performance of high-concentration erbium-doped fiber amplifiers. *IEEE Photonics Technology Letters*, *11*(8), 973–975. (1999).

[11] Ellmer, K., & Wendt, R. D.c. and r.f. (reactive) magnetron sputtering of ZnO:Al films from metallic and ceramic targets: a comparative study. *Surface and Coatings Technology*, *93*(1), (1997). 21–26.